

Compton-y distortion: CMB constraints and new prospects with CIB

Alina Sabyr

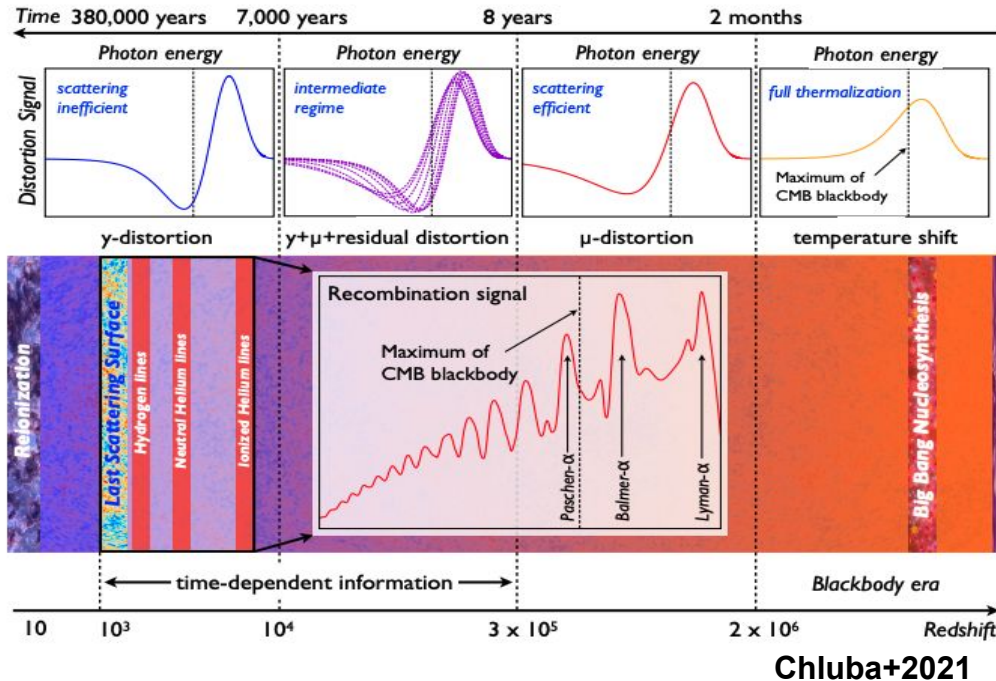
with J. Colin Hill, Giulio Fabbian, Federico Bianchini, Boris Bolliet



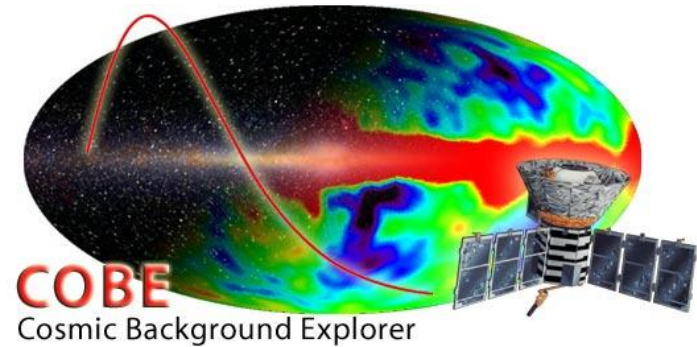
Spectral distortions →
probe the Universe's **thermal** history

$|\langle y \rangle| < 15 \times 10^{-6}$ and $|\langle \mu \rangle| < 90 \times 10^{-6}$ (Fixsen+1996)

$|\langle \mu \rangle| < 47 \times 10^{-6}$ (Bianchini & Fabbian 2022)



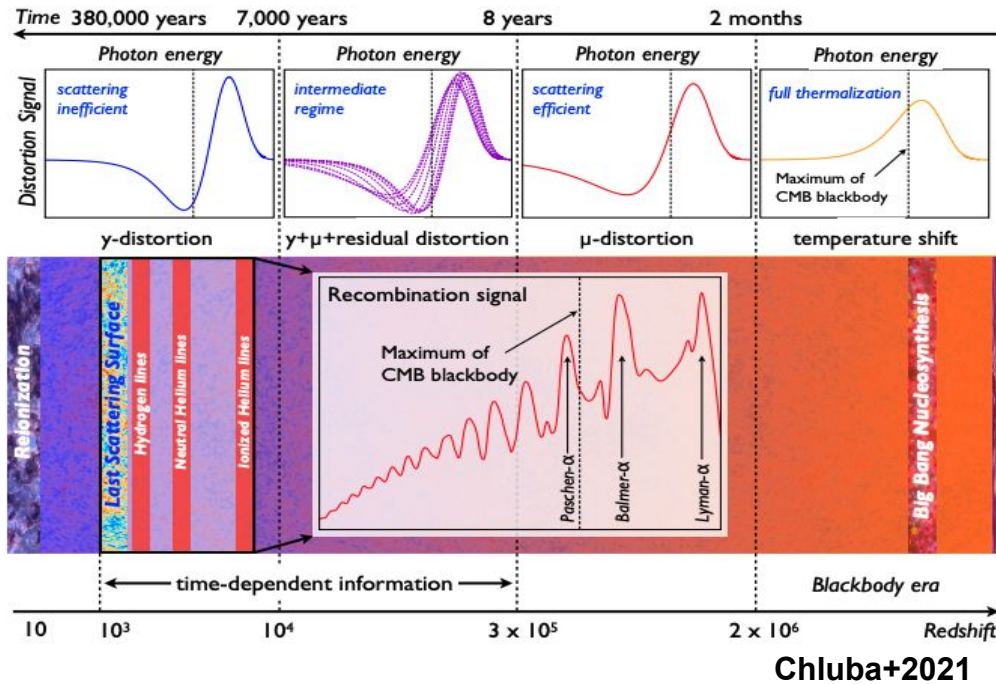
Spectral Distortions



Spectral distortions →
probe the Universe's **thermal** history

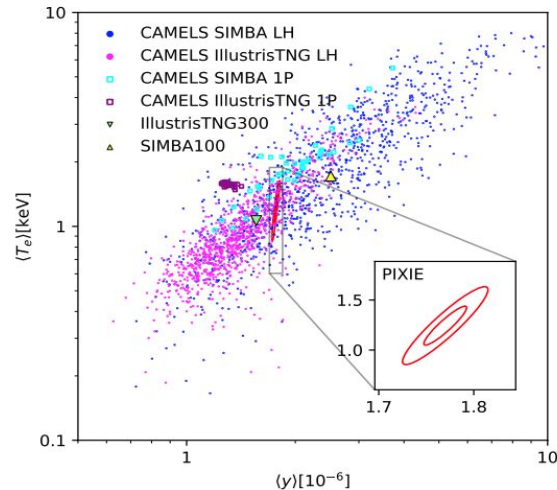
$|\langle y \rangle| < 15 \times 10^{-6}$ and $|\langle \mu \rangle| < 90 \times 10^{-6}$ (Fixsen+1996)

$|\langle \mu \rangle| < 47 \times 10^{-6}$ (Bianchini & Fabbian 2022)



Spectral Distortions

y-distortion: total thermal energy stored in electrons



Thiele+2022

from theory: $y \sim 2 \times 10^{-6}$ (e.g. Hill+2014)

FIRAS Re-Analysis

Main motivation: **validate current forecasting methods** (e.g. PIXIE, Voyage 2050) + **tighten current constraints** on y -distortion (see Bianchini & Fabbian 2022 for pixel-by-pixel μ -distortion analysis)

FIRAS Re-Analysis

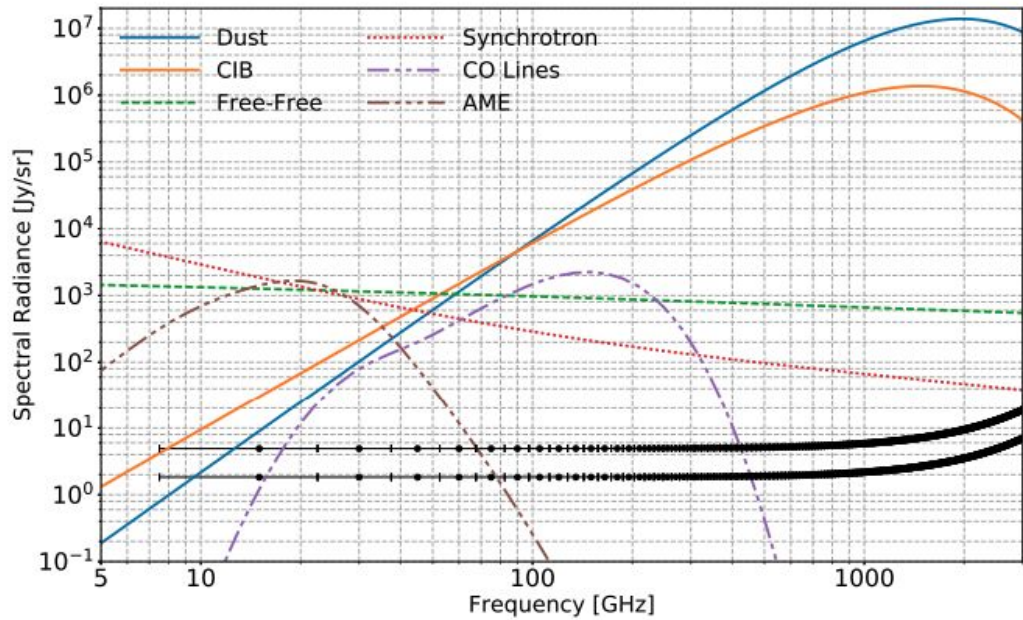
Main motivation: validate current forecasting methods (e.g. PIXIE, Voyage 2050) + tighten current constraints on y -distortion (see Bianchini & Fabbian 2022 for pixel-by-pixel μ -distortion analysis)

Key ingredients:

1. Sky model:

$$\Delta I_\nu = \Delta B_\nu + \Delta I_\nu^y + I_\nu^{\text{fg}}$$

y-distortion
Tcmb deviation **foregrounds**



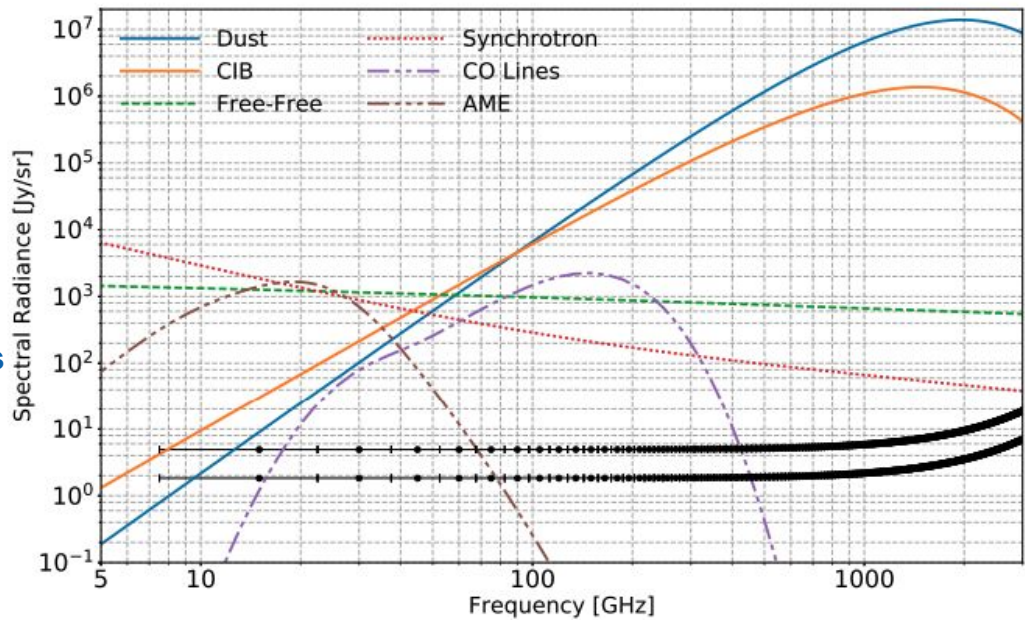
FIRAS Re-Analysis

Main motivation: validate current forecasting methods (e.g. PIXIE, Voyage 2050) + tighten current constraints on γ -distortion (see Bianchini & Fabbian 2022 for pixel-by-pixel μ -distortion analysis)

Key ingredients:

1. Sky model:
2. FIRAS Covariance:

$$C_{\nu p \nu' p} = C^{\nu \nu'} \left(\delta^{pp'} / N_p + \beta_k^p \beta_{p' k} + 0.04^2 \right) \text{ noise}$$
$$+ S^{\nu \nu'} S^{p' \nu'} \left(J^\nu J^{\nu'} + G^\nu G^{\nu'} \delta^{\nu \nu'} \right) \text{ gain error}$$
$$+ P^\nu P^{\nu'} \left(U^2 \delta^{pp'} / N_p + T^2 \right) \text{ systematics}$$



FIRAS Re-Analysis

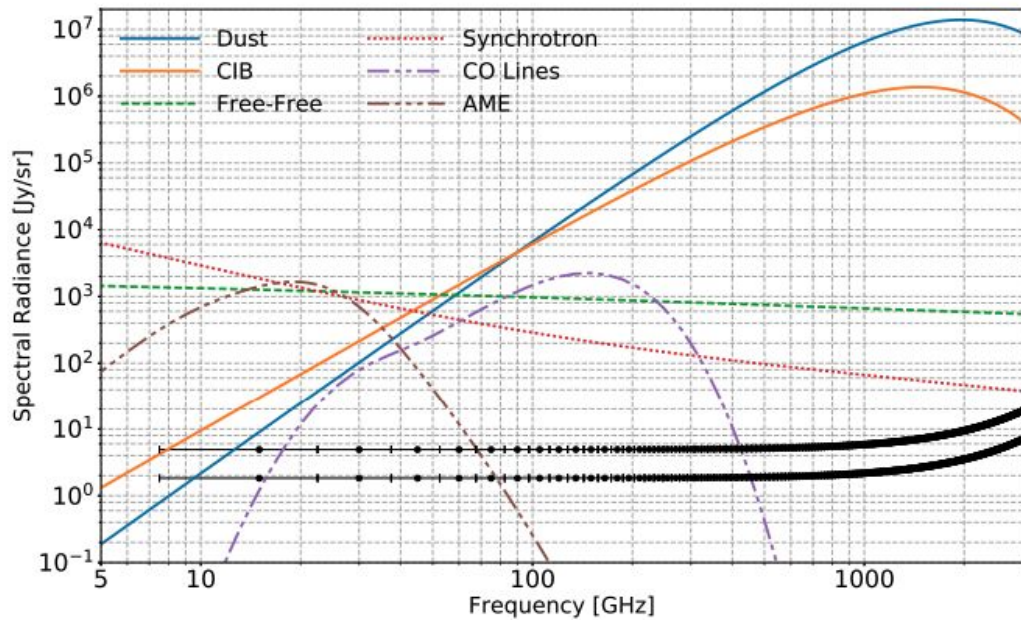
Main motivation: validate current forecasting methods (e.g. PIXIE, Voyage 2050) + tighten current constraints on γ -distortion (see Bianchini & Fabbian 2022 for pixel-by-pixel μ -distortion analysis)

Key ingredients:

1. Sky model:
2. FIRAS Covariance:
3. CMB monopole data:

Low: ~61-650 GHz (43 channels)

High: ~605-2918 GHz (170 channels)



Mock Data Tests (Preliminary)

sky model: $\Delta_T + y + \text{dust}$

inv_var, up to 1.89 THz, fsky=20, orth. stripes True

fsky=40, orth. stripes True

False

fsky=60, orth. stripes True

False

low only, fsky=20, orth. stripes True

False

fsky=40, orth. stripes True

False

fsky=60, orth. stripes True

False

Constant Dust

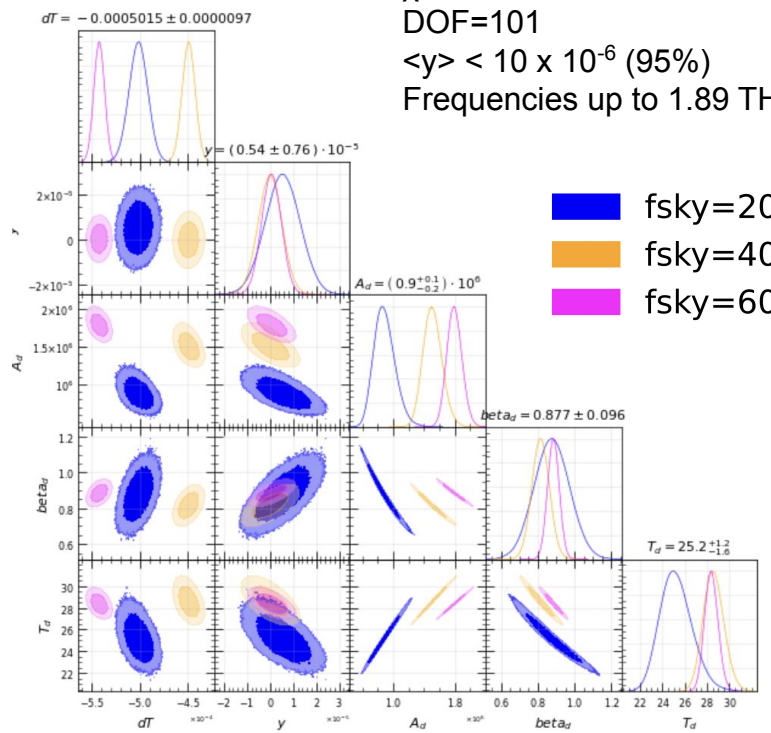
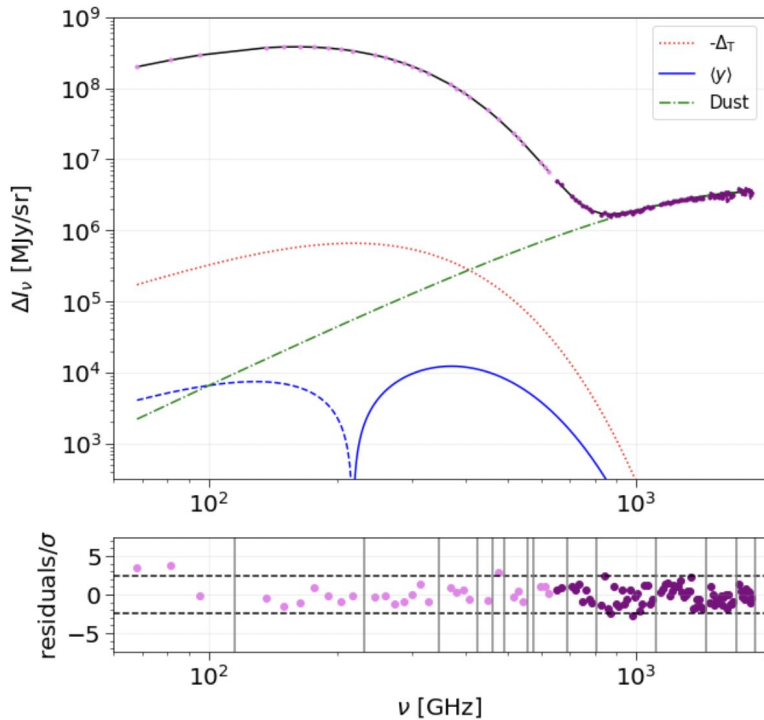


Synch + CO + FF + AME + CIB + Dust

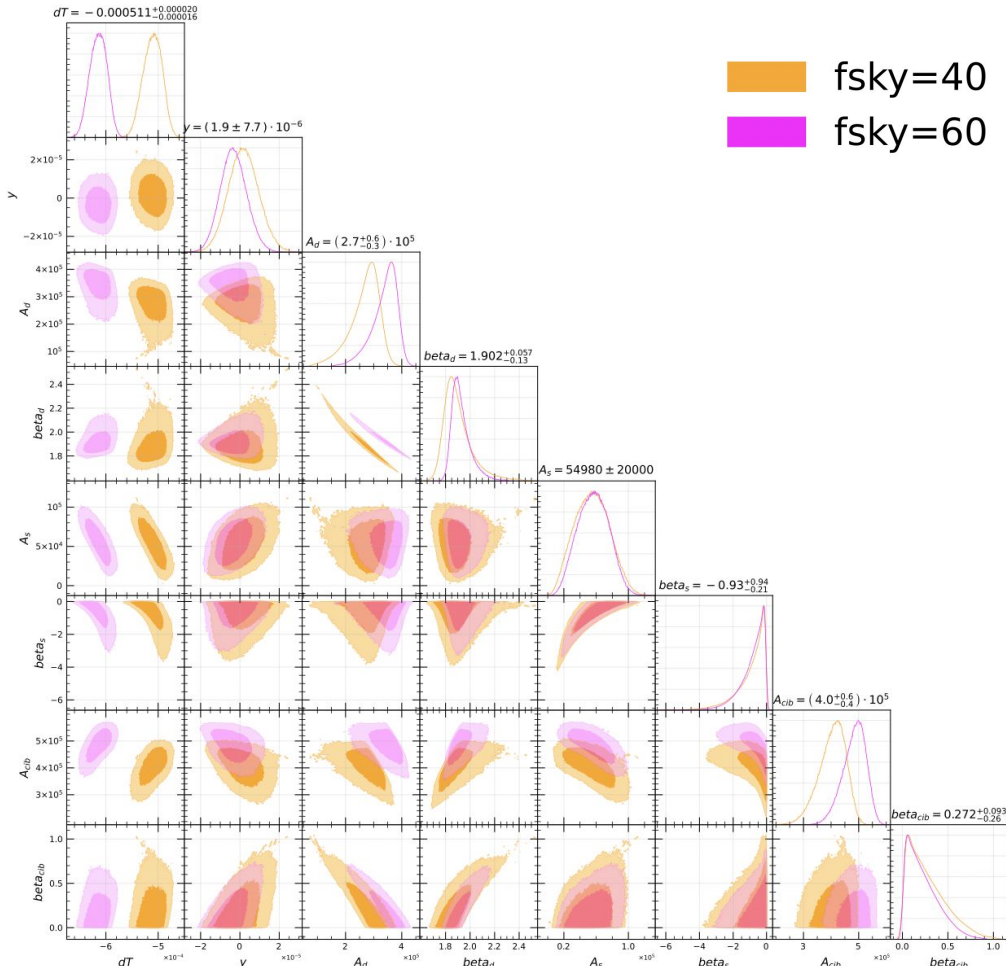


**"orth. stripes" refers to method used for correction of residual instrumental effects.

Results from Data (Preliminary)



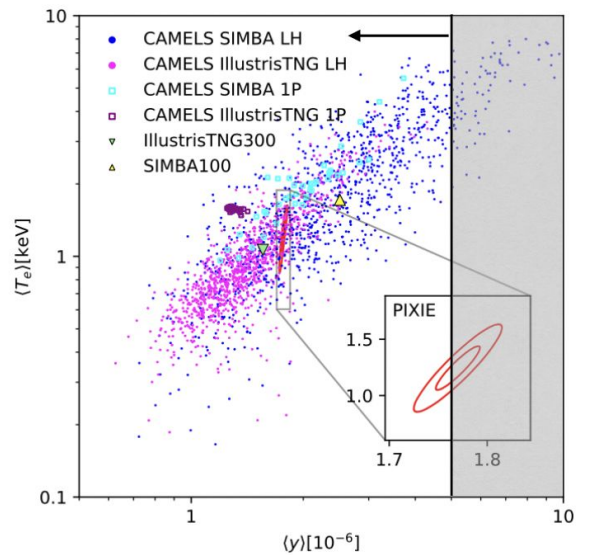
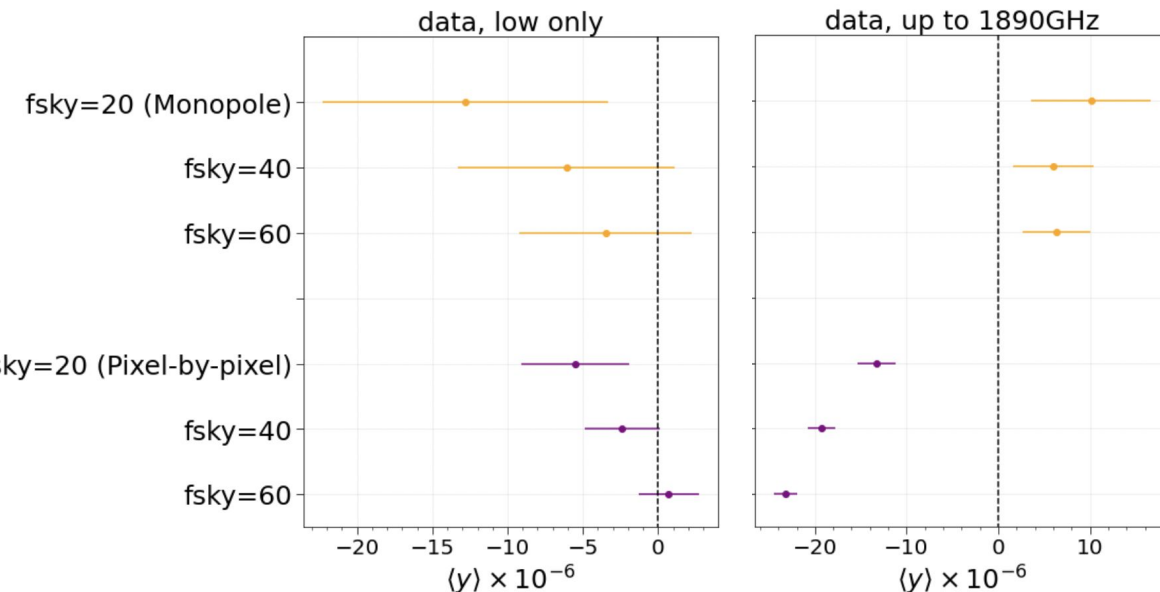
*Note: variability in dT is due to different sky masks



sky model:
 $\Delta_T + y + \text{dust} + \text{synch} + \text{cib}$
 (fixed T_d & T_{cib})

*Note: variability in dT is due to different sky masks

Method and Fisher Forecast Comparison (Preliminary)

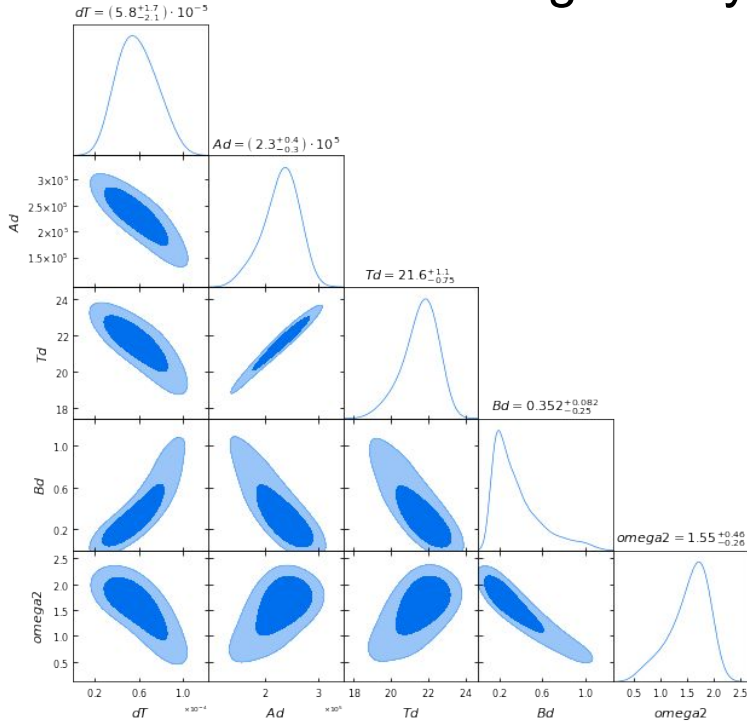


Plot thanks to Giulio & Leander

sky model: $\Delta_T + y + \text{dust}$

up to 1.89 THz , Fisher error ($fsky=60$) $\sim 18 \times 10^{-6}$
monopole $\sim 3.7 \times 10^{-6}$
pixel-by-pixel $\sim 2 \times 10^{-6}$ (low only)

- + consider moment expansion for foregrounds to fit higher sky fractions (in progress)



$\Delta_T, \langle y \rangle, 0 < A_d, 0 < \beta_d < 3, 0 < T_d < 100$	fsky=20	fsky=40	fsky=60
ν_{THz}	1.7	2.6	3.6
$\nu_{1.89\text{THz}}$	1.5	2.3	3.5
$\Delta_T, \langle y \rangle, 0 < A_d, 0 < \beta_d < 3, 0 < T_d < 100, \omega_2, \omega_3$	fsky=20	fsky=40	fsky=60
ν_{THz}	1.5	2.3	3.1
$\nu_{1.89\text{THz}}$	1.3	2.0	3.0

$$\langle I_\nu \rangle = \bar{A}_0 \frac{(\nu/\nu_0)^{\bar{\alpha}} \nu^3}{e^x - 1} \left\{ 1 + \omega_2 \ln(\nu/\nu_0) + \omega_3 \frac{x e^x}{e^x - 1} \right\}$$

Moment approach from Chluba, Hill & Abitbol 2017

Inverse-Compton scattering of the cosmic infrared background (CIB)

(Sabry, Hill, & Bolliet 2022, arXiv:2202.02275)

CIB:

- Thermal **dust emission** in **star-forming** galaxies.
- Generated during **late universe**.

Use halo model prescription from

Sheng+2012, McCarthy & Madhavacheril 2021:

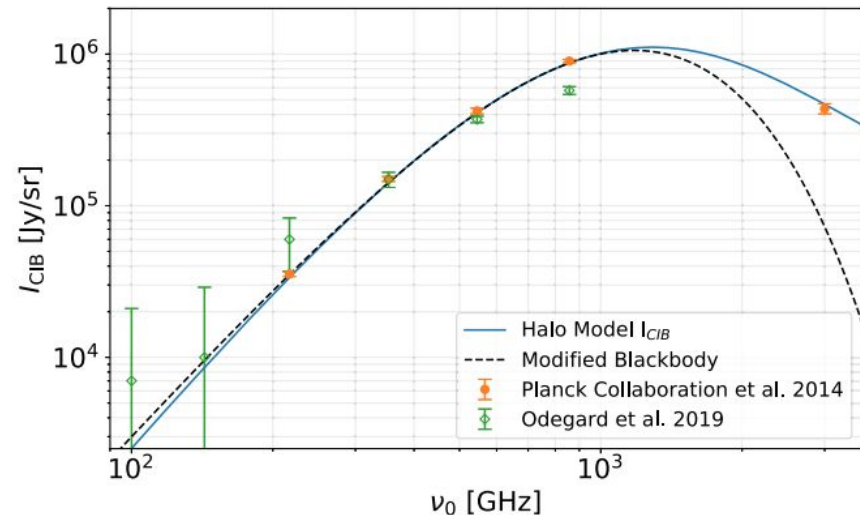
$$L_{\nu}^{\text{gal}}(M, z) = L_0 \Phi(z) \Sigma(M) \Theta(\nu, z)$$

Galaxy luminosity

Redshift evolution $(1+z)^{0.36}$

SED: Modified blackbody at low ν , power law at high ν

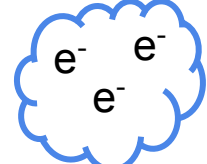
Luminosity-mass relation: Log-normal distribution



Integrate over all halos & redshift to get the monopole

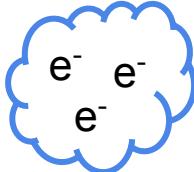
implemented in **class_sz**, https://github.com/borisbolliet/class_sz
<https://github.com/CLASS-SZ>

$$\int_{z=1}^{\infty} \frac{dI_{\text{CIB}}}{dz} dz$$



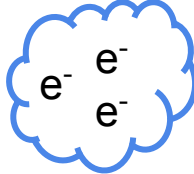
$z = 1$

$$\int_{z=2}^{\infty} \frac{dI_{\text{CIB}}}{dz} dz$$



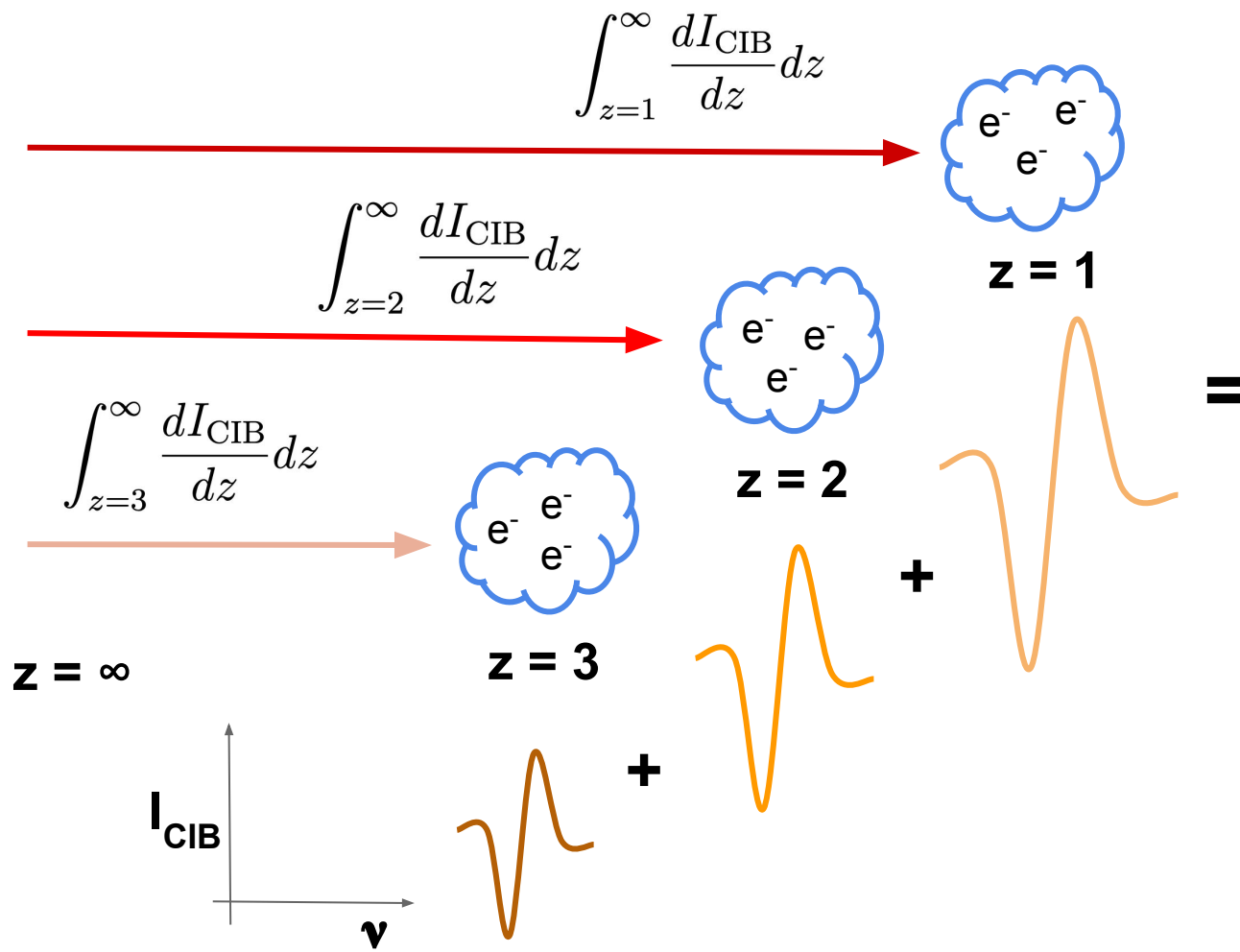
$z = 2$

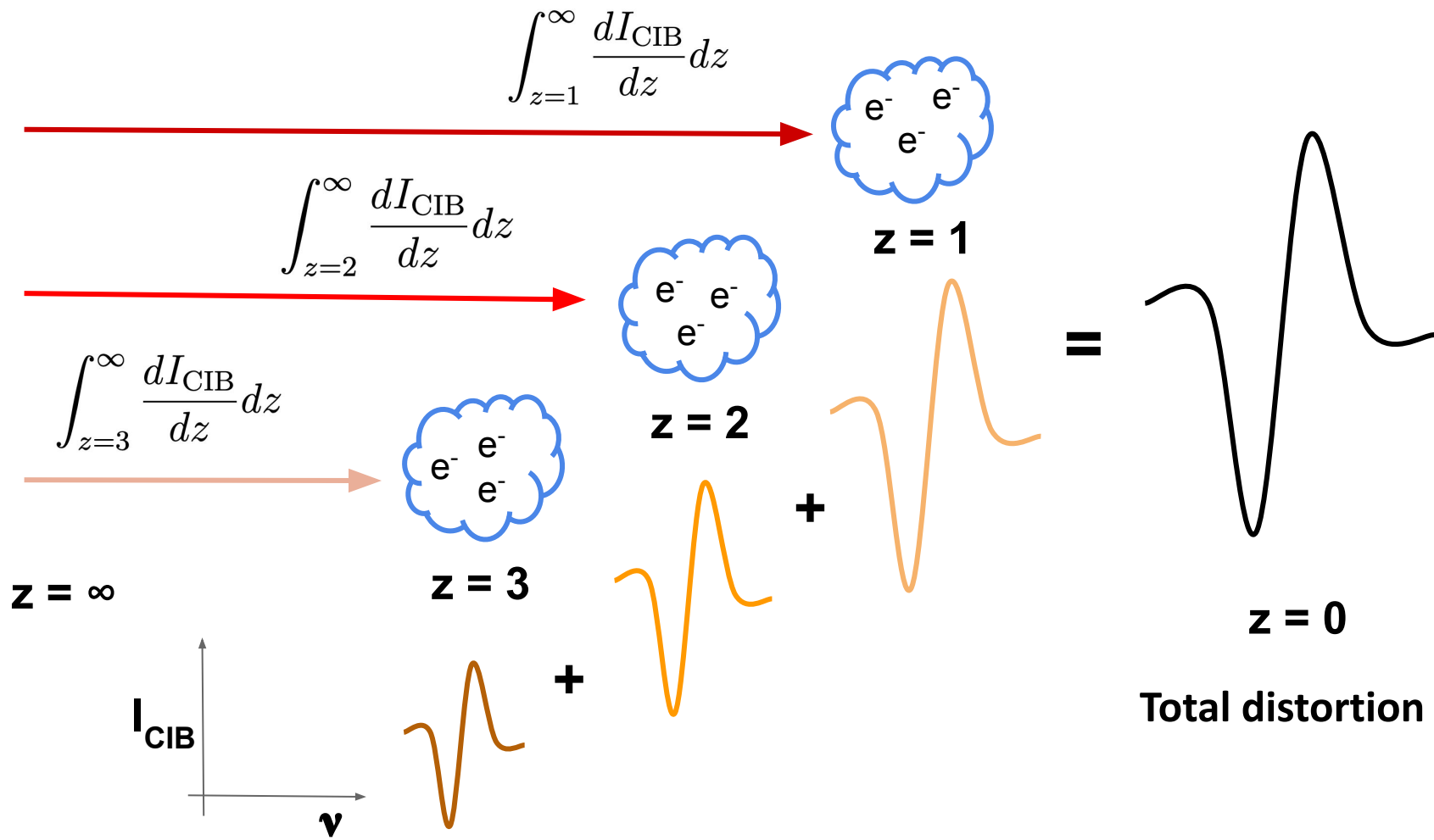
$$\int_{z=3}^{\infty} \frac{dI_{\text{CIB}}}{dz} dz$$

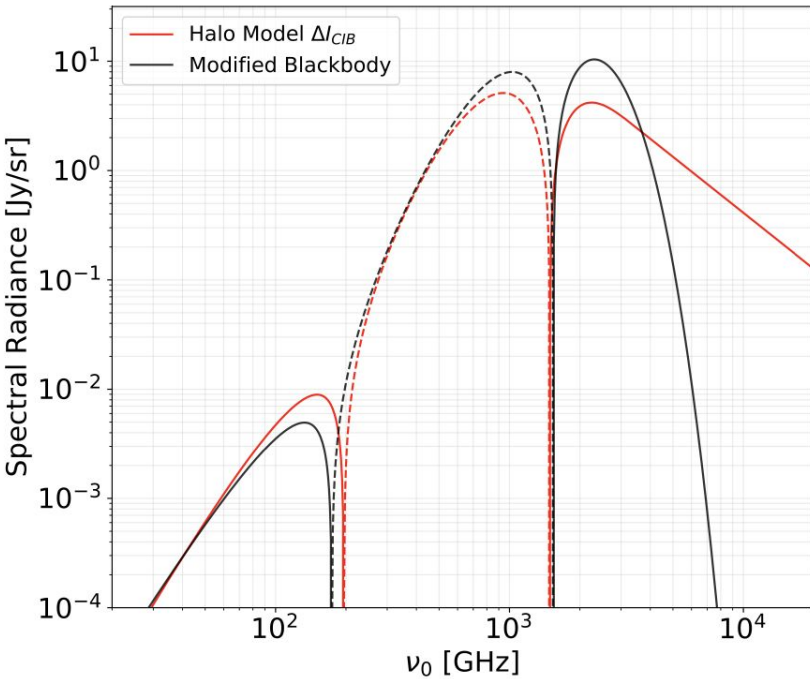


$z = 3$

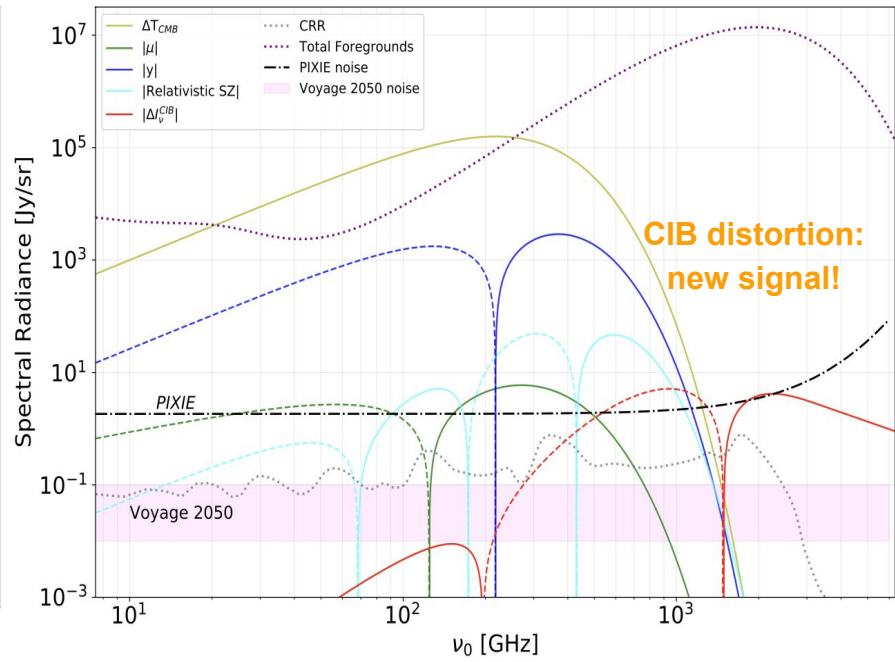
$z = \infty$







~4 Jy/sr (-5 Jy/sr) at 2260 GHz (940 GHz)



Null frequencies at 196 and 1490 GHz.

Fisher forecast (including all foregrounds):

PIXIE: $\sim 0.1\sigma$

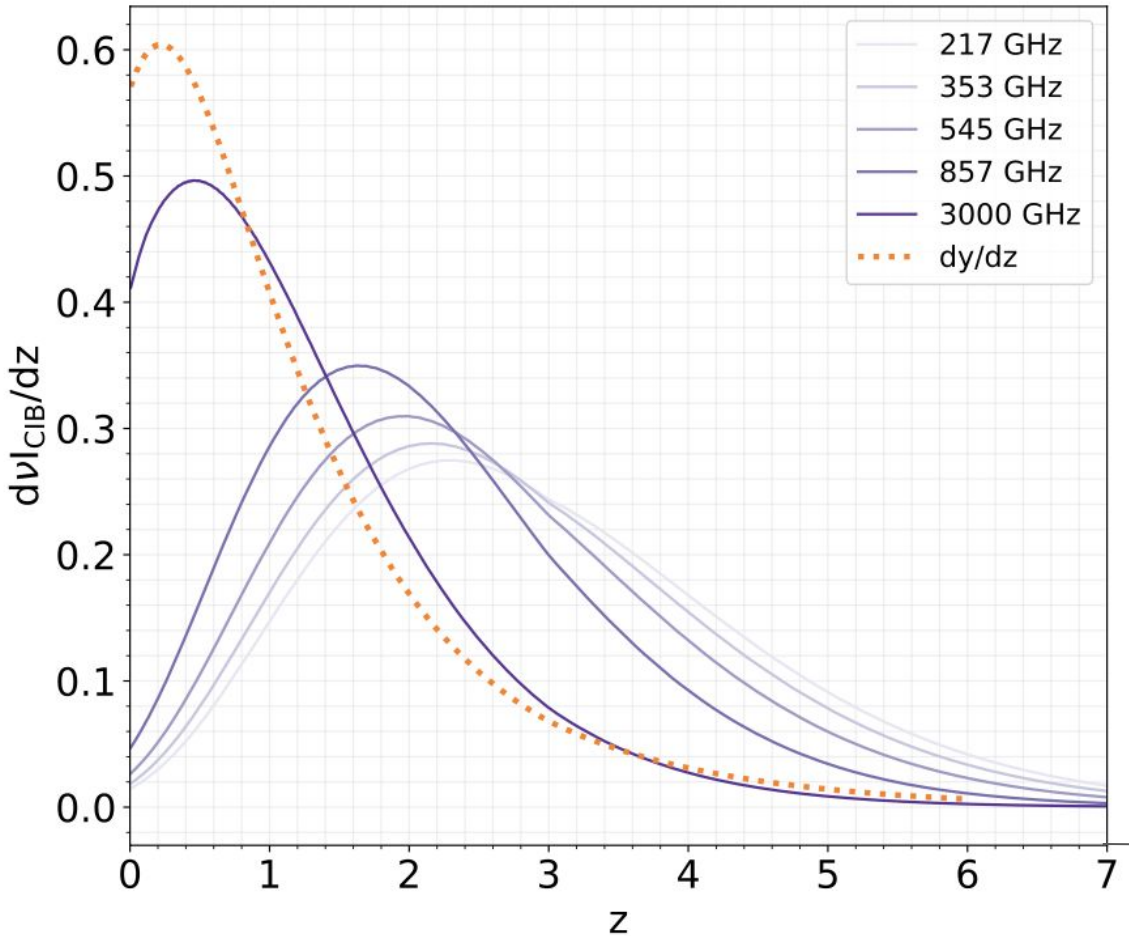
ESA Voyage 2050: $\sim 0.9\text{-}4.6\sigma$

Relativistic & intracluster effects: see Acharya & Chluba 2022.

Summary

- FIRAS re-analysis allows us to asses our **models, analysis techniques, and accuracy of forecasts** for future missions and tighten upper bounds by a **factor of ~2-3**.
 - ◆ Noise characterization is crucial to take full advantage of future CMB measurements.
 - ◆ Pixel-by-pixel and monopole methods offer different advantages.
- Analogue tSZ distortion in the CIB – a **new signal** in the infrared sky and a tool to study the **star formation history!**
 - ◆ Detection with Voyage 2050 is possible but **targeted observations of clusters & anisotropy experiments** may provide measurements sooner (e.g. Coma cluster with $y \sim 6 \times 10^{-4}$ (Planck+2013); stacking analysis with CCAT-prime + SO)

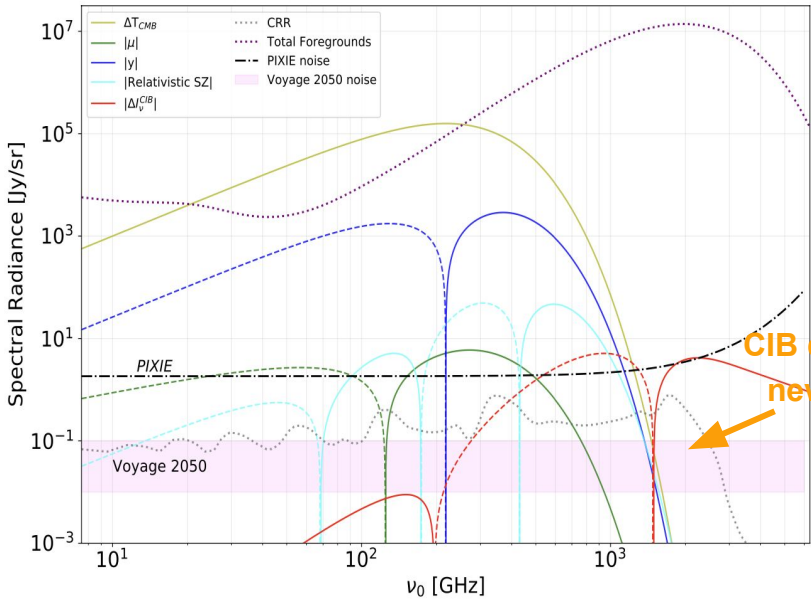
Extra Slides



CIB primarily originates
z $\sim 1 - 6$

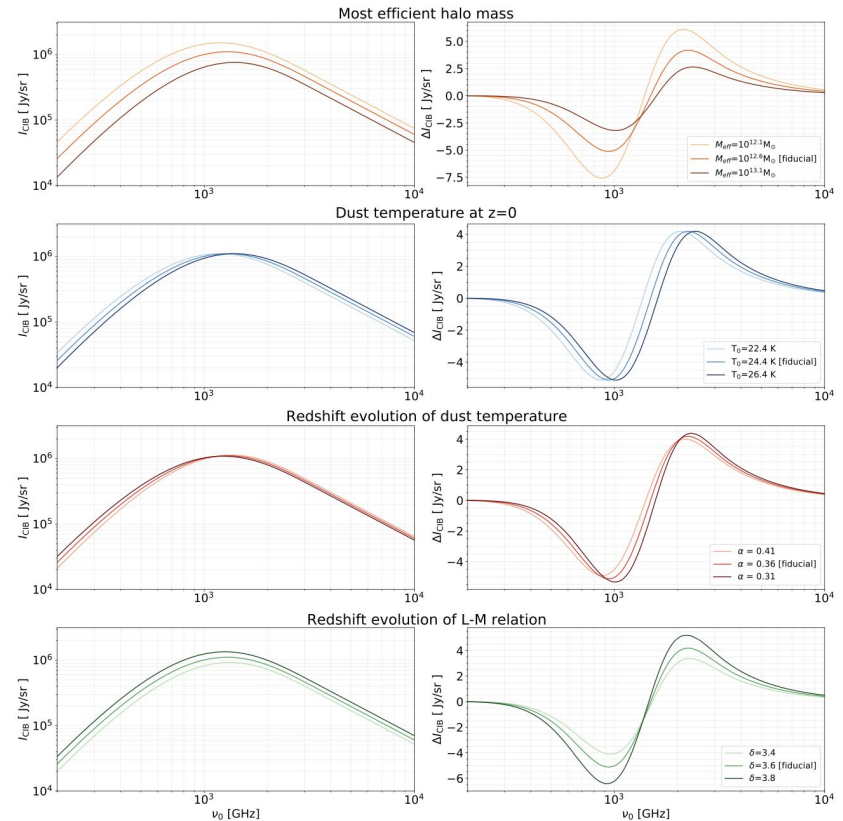
Compton-y at
z $\lesssim 2$

*Battaglia+2010 pressure profile & Tinker+10 halo mass function



CIB alone:
 PIXIE: 3.6σ
 ESA Voyage 2050: $73\text{-}364\sigma$

with all foregrounds:
 PIXIE: 0.1σ
 ESA Voyage 2050: $0.9\text{-}4.6\sigma$



Distortion's sensitivity to **halo model parameters**.

Cosmic Infrared Background (CIB)

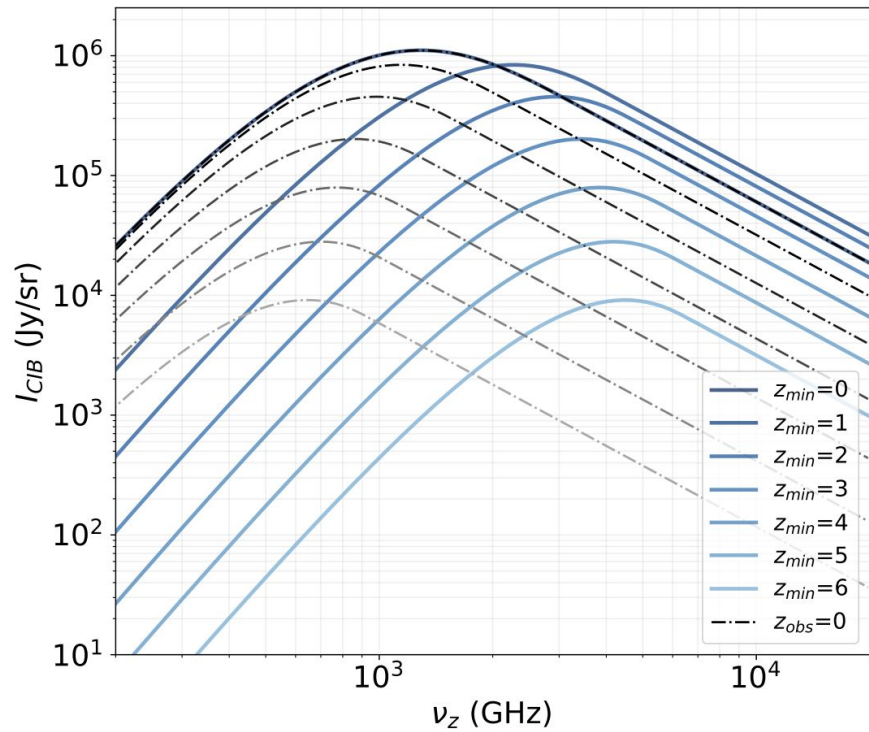
Integrate over all halos
(comoving emissivity)

$$\tilde{j}_{\nu_z}(z') = \int_{M_{\min}}^{M_{\max}} dM \frac{dN}{dM} \frac{1}{4\pi} \frac{L_{\frac{(1+z')}{(1+z)}\nu_z}(M, z')}{4\pi}$$

Integrate over redshift
(comoving specific intensity)

$$\tilde{I}_{\nu_z}^{\text{CIB}}(z) = \int_z^{z_{\max}} dz' \frac{\tilde{c}j_{\nu_z}(z')}{(1+z')H(z')}$$

Implemented in **class_sz**,
https://github.com/borisbolliet/class_sz
<https://github.com/CLASS-SZ>



Inverse-Compton Scattering

- Use Kompaneets approximation (**Kompaneets 1957**)
 - ◆ Non-relativistic, $T_e \gg T_{cib}$ and $y \ll 1$

$$\Delta N(\nu) \approx \frac{y}{\nu^2} \frac{\partial}{\partial \nu} \left[\nu^4 \frac{\partial N(\nu)}{\partial \nu} \right]$$

Compton-y
↓
**photon occupation
number**
↑

- Calculate differential distortion at each infinitesimal redshift & add up.

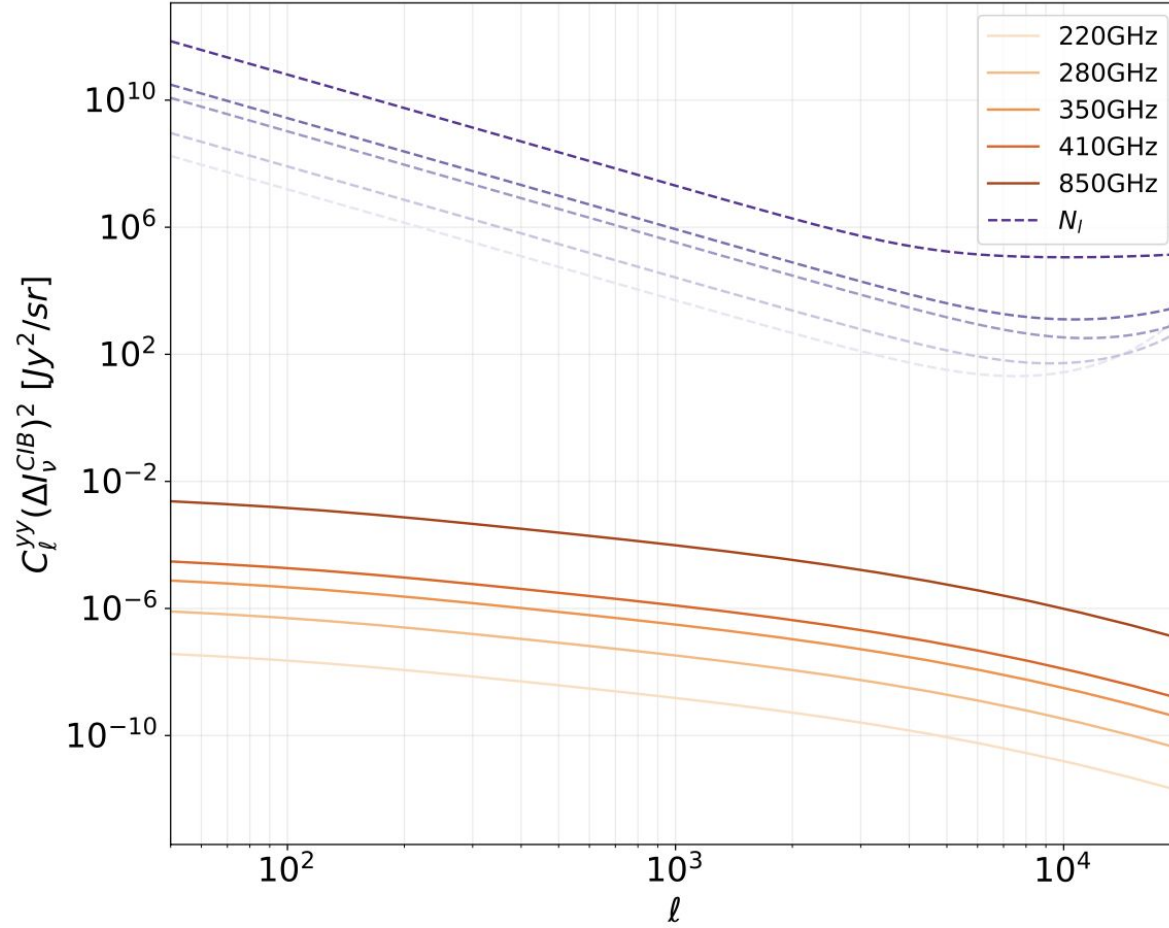
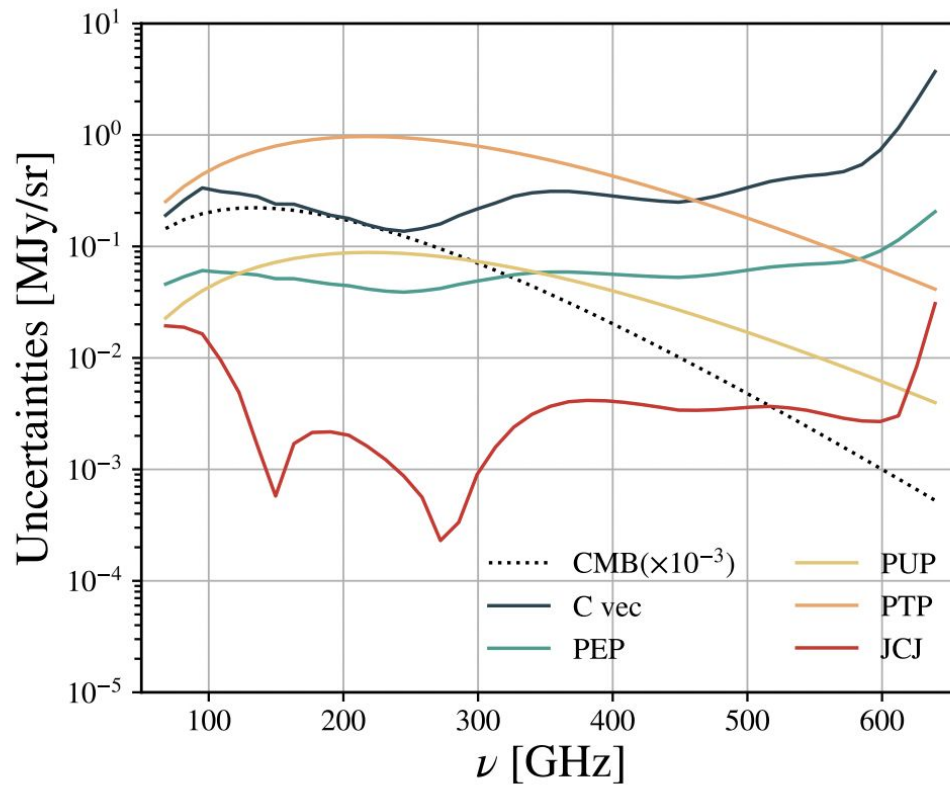


Table 9. Mean values and marginalized 68% CL for halo model parameters and shot-noise levels (in Jy² sr⁻¹).

Parameter	Definition	Mean value
α	SED: redshift evolution of the dust temperature	0.36 ± 0.05
T_0 [K]	SED: dust temperature at $z = 0$	24.4 ± 1.9
β	SED: emissivity index at low frequency	1.75 ± 0.06
γ	SED: frequency power law index at high frequency	1.7 ± 0.2
δ	Redshift evolution of the normalization of the L - M relation	3.6 ± 0.2
$\log(M_{\text{eff}}/M_\odot)$	Halo model most efficient mass	12.6 ± 0.1
$M_{\min}[M_\odot]$	Minimum halo mass	unconstrained
$S^{3000 \times 3000}$	Shot noise for 3000 GHz \times 3000 GHz	9585 ± 1090
$S^{3000 \times 857}$	Shot noise for 3000 GHz \times 857 GHz	4158 ± 443
$S^{3000 \times 545}$	Shot noise for 3000 GHz \times 545 GHz	1449 ± 176
$S^{3000 \times 353}$	Shot noise for 3000 GHz \times 353 GHz	411 ± 48
$S^{3000 \times 217}$	Shot noise for 3000 GHz \times 217 GHz	95 ± 11
$S^{857 \times 857}$	Shot noise for 857 GHz \times 857 GHz	5364 ± 343
$S^{857 \times 545}$	Shot noise for 857 GHz \times 545 GHz	2702 ± 124
$S^{857 \times 353}$	Shot noise for 857 GHz \times 353 GHz	953 ± 54
$S^{857 \times 217}$	Shot noise for 857 GHz \times 217 GHz	181 ± 6
$S^{545 \times 545}$	Shot noise for 545 GHz \times 545 GHz	1690 ± 45
$S^{545 \times 353}$	Shot noise for 545 GHz \times 353 GHz	626 ± 19
$S^{545 \times 217}$	Shot noise for 545 GHz \times 217 GHz	121 ± 6
$S^{353 \times 353}$	Shot noise for 353 GHz \times 353 GHz	262 ± 8
$S^{353 \times 217}$	Shot noise for 353 GHz \times 217 GHz	54 ± 3
$S^{217 \times 217}$	Shot noise for 217 GHz \times 217 GHz	21 ± 2



Bianchini & Fabbian 2022